

Modeling and Measurement of Amplitude Dependent Tune Shifts in the Cornell Electron Storage Ring

Sarah K. Woodall

Department of Biology, Lander University, Greenwood, SC, 29649

(Dated: August 13, 2010)

The amplitude dependent tune shifts of the Cornell Electron Storage Ring (CESR) originate as a product of the action of sextupole magnets on the beam within the CESR lattice. In order to study the amplitude dependence of the horizontal and vertical tune shifts, simulations were used to model turn-by-turn data for a variety of amplitudes in two family sextupole distributions in the lattice and in optimized versions of those two family sextupole distributions. By taking actual CESR turn-by-turn measurements for different amplitudes with one of the simulated sextupole distributions, the model and CESR measurements can be compared to see the accuracy of the model.

I. INTRODUCTION

The non-linear lattice of CESR is composed of several different types of magnets for controlling the electron and positron beams by bending, steering, and focusing them along with other components that control other aspects of the beam. While dipole magnets are used for bending the beam through the beam pipe, the quadrupole magnets are used for beam focusing and are responsible for the oscillation of the beam as it moves through the ring. The two types of quadrupole magnets are F quadrupoles and D quadrupoles. F quadrupoles focus the beam in the horizontal plane and defocus in the vertical plane while D quadrupoles focus vertically and defocus horizontally. Alternately placed throughout the ring, the action of the F and D quadrupoles on the beam results in a net focusing effect and the oscillation of the beam.

The tune, Q , is the number of oscillations that the beam experiences about its central axis as it passes through the beam pipe in a single turn. Tune is defined as: [2]

$$Q = \frac{1}{2\pi} \oint \frac{ds}{\beta(s)} \quad (1)$$

As the focusing strength of the quadrupole magnets increases, the tune increases. This is because the beam size, and thus the Beta function, get smaller as the focusing strength increases. Because tune is dependent on the inverse of the Beta function, it increases as Beta decreases.

As the particles within the beam pass around the ring, they will experience a transverse kick from the quadrupole magnets that is proportional to the displacement of the particle from the central axis of the beam. The farther away the particle is from the central axis, the larger the kick is from the quadrupoles. This keeps the tune independent of the amplitude and makes the beam act as a simple harmonic oscillator. The sextupole magnets within the lattice are necessary for the correction of beam energy spread. Because the kick from the sextupoles is non-linear, this results in the tune of the beam becoming amplitude dependent.

II. METHOD OF INVESTIGATION

Because the data taken from CESR would be in the form of position data, I used the Python programming language to create scripts which would extract frequency and tune from position data. Because frequency is the number of oscillations in an amount of time and tune is the number of oscillations in one turn, which is approximately 2.5 microseconds in CESR, tune can be found similarly to frequency by adjusting for the amount of time in one turn.

A. Non-Linear Oscillator Model

In order to become more familiarized with the process of calculating the period and frequency from position data, I first worked with position data from a simple pendulum, a non-linear oscillator.

1. Local Maxima Method

Position data for the pendulum was calculated after numerical integration of the differential equation:

$$\frac{d^2\theta}{dt^2} = -\sin\theta \quad (2)$$

After plotting position versus time, the average period was calculated by locating the local maxima of the position data and finding the period between those peaks. One maximum to the next constitutes a full oscillation; thus the period is the time between peaks and the frequency can be found as its inverse. The period of the pendulum motion was checked against the analytical solution for small angles using the small angle approximation. [1]

2. Fast Fourier Transform

The periodicity of the pendulum motion allows for it to be analyzed through Fourier analysis. With a Fast Fourier Transform (FFT), the position data recorded from the pendulum was transformed into frequency data. By analyzing the frequency spectrum created by the FFT, the dominant frequency from the position data can be found by looking for the frequency with the largest amplitude in the FFT. The FFT is a useful tool because in Python it is a much faster way to analyze the position data and find the frequency than using the local maxima method.

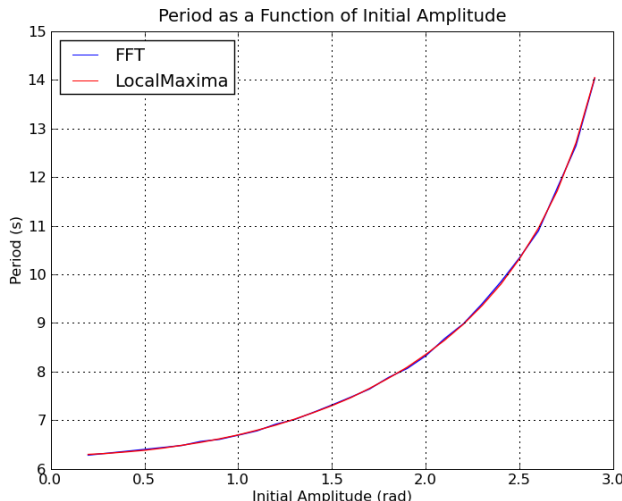


FIG. 1: Using both the local maxima and FFT methods, the periods and frequencies for a range of initial amplitudes were found for the non-linear oscillator model.

With using both the local maxima method and FFT for finding the period and frequency of an oscillation and comparing the two methods in Fig. 1, it is apparent that both are working correctly and are in good agreement with each other.

B. Simulations

Turn-by-turn data for CESR was simulated using an object-oriented subroutine library called Bmad. Horizontal and vertical positions of one bunch were simulated for 1024 turns at one Beam Position Monitor (BPM) within the lattice. Simulations were done for four CESR lattices with 4-dimensional and 6-dimensional tracking. The first two lattices are based on a two family distribution of sextupoles, where the two families alternate throughout the ring with one family having positive values and the other family having negative values. The specific values for each sextupole family are different and dependent upon correcting for off energy beam spread or chromaticity. The latter two sextupole distributions are optimized versions of the first two lattices which correct for chromaticity and amplitude dependent tune shift while also reducing various resonance-driving terms. The sextupole values for these optimized lattices are different for each sextupole on the east and west sides of the ring, while symmetric between the two sides.

For each sextupole distribution, a matrix of horizontal and vertical amplitudes was used to create the position data. Initially, simulations were taken with initial amplitudes up to 20mm from the central axis of the beam in the horizontal and vertical planes. However, beam instabilities were prevalent at higher amplitudes, so the simulations were then narrowed to a range of amplitudes from .1 mm to 10 mm in x and y. This allowed for the observation of the beam's tune shift within the dynamic aperture, where the beam is stable.

By taking an FFT of the position data, the horizontal and vertical tunes can be found at each amplitude in each lattice. The tune shift for each amplitude is calculated by subtracting the zero-amplitude tune from the tune at that amplitude, where the zero-amplitude tunes for each lattice were the tunes calculated with initial horizontal and vertical amplitudes

of .1 mm. The horizontal zero-amplitude tunes were approximately .570 and the vertical zero-amplitude tunes were approximately .629, with slight variations between lattices.

For each sextupole distribution, the amplitude dependence of the horizontal tune shift was found by fitting a quadratic equation to the x tune shift versus a range of x amplitudes when the y amplitude was .1 mm, with the amplitude dependence of the vertical tune shift being found similarly. The quadratic coefficient in the quadratic equation that was fit to the data shows the amplitude dependence of the tune shift, with larger numbers being more amplitude dependent and smaller numbers being less amplitude dependent.

Amplitude Dependence of Tune Shift				
Lattice Name (cta_2085mev)	20090516	20090516_newsext	xr20m_20091205	xr20m_20091205_newsext
Lattice Type	Two Family	Optimized	Two Family	Optimized
6d Tracking				
Amp Dep of dQx	3.027E+02	2.729E+01	1.138E+02	2.203E+01
Amp Dep of dQy	3.461E+02	2.874E+02	2.760E+02	2.583E+02
4d Tracking				
Amp Dep of dQx	3.113E+02	0.000E+00	1.237E+02	2.678E+01
Amp Dep of dQy	3.465E+02	2.874E+02	2.800E+02	2.584E+02

FIG. 2: The table shows the values for dependence of tune shift on amplitude for the four separate lattices used in the simulations.

As seen in Fig. 2, differences between 4d and 6d tracking are minimal. In order to compare simulation data with CESR machine studies data, 6d tracking was used to make the simulation as realistic as possible.

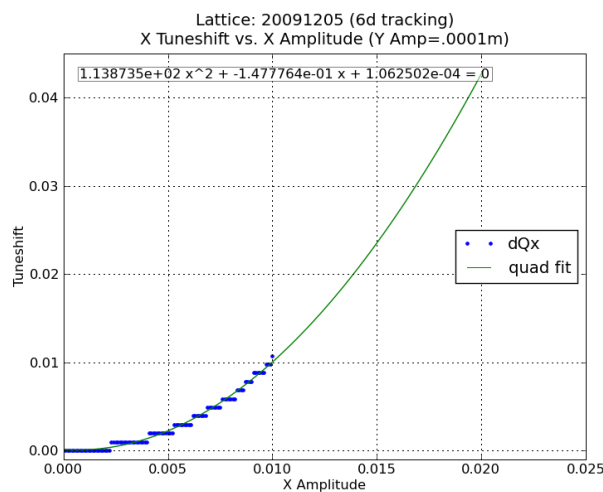


FIG. 3: This is an example of finding the amplitude dependence of the tune by fitting a quadratic equation to the simulation data for x tune shift in a two family sextupole distribution.

In Fig. 3, the tune shifts of the simulation are quantized and appear in a stepped fashion. This is due to the nature of the FFT because the resolution of the FFT is limited to the inverse of the number of data points it was used for. In this case, by taking an FFT of position data from 1024 turns, the FFT resolution is .00097, or 1/1024, which is the step size between quantized tune shifts in the figure. This presents a problem in the 4d tracking

for the 20090516_newsext optimized sextupole distribution from Fig. 1 because dependence of the tune shift on amplitude in the horizontal has been decreased so much that the tunes the FFT finds for the different amplitudes are all the same. If the resolution of the FFT were better, this would not be a problem when determining the amplitude dependence of the tune shift.

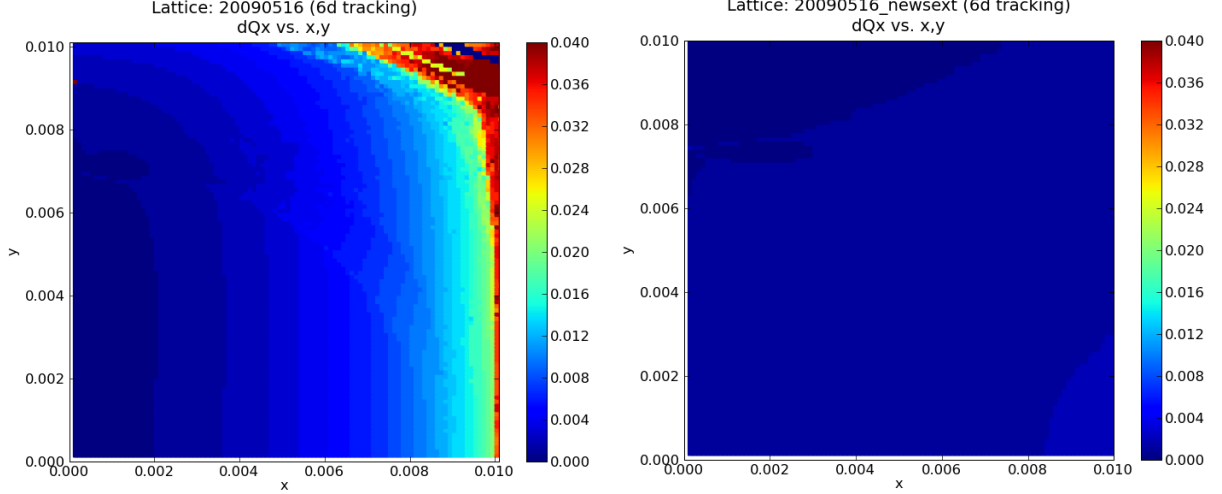


FIG. 4: These are plots showing the change in horizontal tuneshifts with respect to x and y amplitudes for a two family sextupole distribution (left) and an optimized sextupole distribution (right).

In comparing the two family and optimized sextupole distributions for the x tune shifts in Fig. 4, it is apparent that the optimized lattice has effectively decreased the amplitude dependence of the x tune shift, as well as correcting the resonance band in the x tune shift from the two family sextupole distribution.

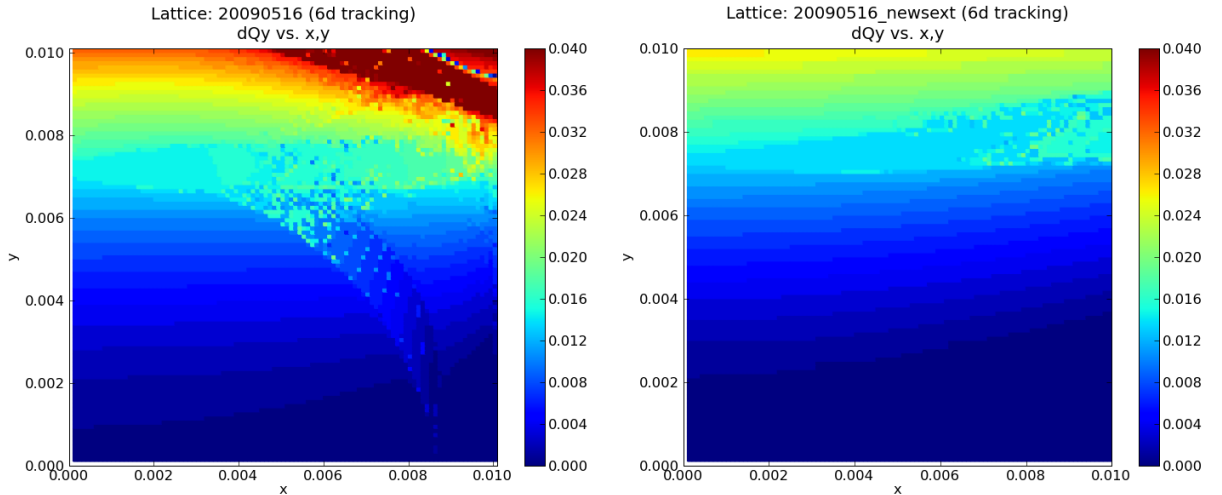


FIG. 5: These are plots showing the change in vertical tuneshifts with respect to x and y amplitudes for a two family sextupole distribution (left) and an optimized sextupole distribution (right).

When comparing the two family and optimized sextupole distributions for the y tune shifts in Fig. 5, the optimized lattice appears to have corrected for the resonance band in the y tune shift from the two family sextupole distribution. However, while the optimized lattice has slightly decreased the amplitude dependence of the y tune shift from the two family lattice, it hasn't decreased the amplitude dependence of the y tune shift nearly to the degree that it did for the x tune shift.

C. CCSR Machine Studies Data

Turn-by-turn data was taken from CCSR for lattice `cta_2085mev_xr20m_20091205`, which is a two family sextupole distribution. Data was collected over all BPMs in the ring for a single bunch for 1024 turns. Different amplitudes for CCSR measurements were created using a horizontal or vertical pinger. A pinger is a magnet that is turned on for a very short amount of time; in this case, as the beam is passing by it, the pinger turns on and off before the beam comes around on its next turn, meaning that it is on for less than 2.5 microseconds. In the time that the pinger is on, the beam gets a kick from the pinger and the turn-by-turn data collection is started right after the kick. The range of amplitudes in the horizontal direction was created by using a horizontal pinger on the beam, increasing the strength of the pinger between runs to create the higher amplitudes needed to take the CCSR measurements. The range of amplitudes in the vertical direction was created similarly using the vertical pinger.

Due to time constraints on the project, a Fortran program was used to find positions and resulting tunes for the CCSR data. With this program in place, there is no quantization of tunes because the FFT was interpolated between data points, allowing for it to find the tune at a much higher resolution.

In order to compare the amplitude dependence of tune between CCSR data and the simulations, the amplitudes needed to be normalized for both the CCSR measurements and the simulation. The normalized amplitudes were found by taking the maximum displacement from the central axis at each BPM and multiplying it by the square root of β at each BPM.

$$x = a\sqrt{\beta} \quad (3)$$

For simulations, amplitudes were normalized using β at L0, where β_x is 4.69 m and β_y is 8.28 m, and the maximum displacements were the amplitudes that were initially used to create the data. For CCSR, the turn-by-turn data was read in using Bmad tracking codes and the amplitudes were normalized based on the amplitude and β at each specific BPM where data was taken.

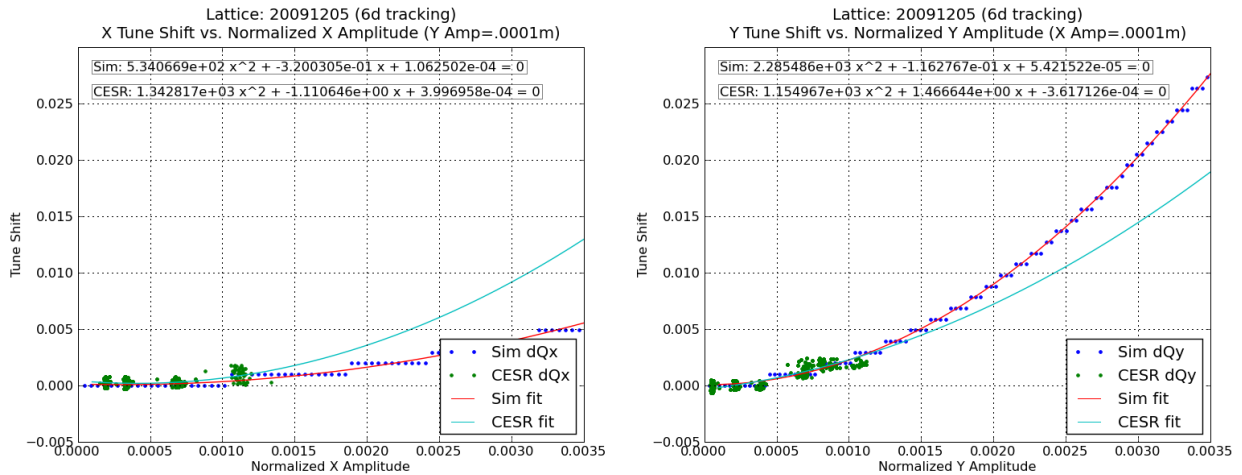


FIG. 6: These plots show CCSR and simulation tune shifts and calculations for the amplitude dependence of the tune shift for a range of horizontal amplitudes (left) and vertical amplitudes (right).

While the calculated amplitude dependences of the tune shift were not in agreement in Fig. 6 between the simulation and the CCSR measurements, the CCSR data does seem to follow the simulation data fairly well when the quadratic equation fit to the CCSR measurements is not taken into account. With uncertainties in CCSR measurements of around .0001 m for normalized amplitude and around .001 for tune shift, there could be some error in the fit of the quadratic equation to the CCSR measurements that was not taken into account.

III. CONCLUSIONS AND SUGGESTIONS FOR FUTURE WORK

The measurements from CCSR are not inconsistent with the model given the uncertainties of finding the amplitude dependence of the tune shift. In order to have a better comparison between the model and the CCSR measurements, larger amplitudes could be used when taking CCSR measurements. Also, CCSR data could be measured for the remaining sextupole distributions that were simulated but had no actual CCSR measurements taken. The accuracy of the model could be improved by using the interpolated FFT to get a better resolution of tunes for the simulations.

Nonlinearities arising from trying to observe the beam at high amplitudes within BPMs were not taken account for in this project; future work could include trying to understand the BPM systematics in order to take more accurate measurements.

Based on the simulations, the optimized sextupole distributions might be further optimized to reduce the amplitude dependence of vertical tune shift.

IV. ACKNOWLEDGMENTS

I would like to acknowledge my mentor David Rubin and graduate student Jim Shanks, both of Cornell University, for their guidance and support on this project. I would also like to thank the CLASSE program and its administrators for making this experience at Cornell

possible for me. This work was supported by the National Science Foundation REU grant PHY-0849885, NSF grant PHY-0734867, and DOE grant DE-FC02-08ER41538.

- [1] F. Blatt, "Principles of Physics," p. 306, Allyn and Bacon, Inc., 1983.
- [2] K. Wille, "The Physics of Particle Accelerators," p. 101, Oxford University Press, 2000.